

A study on the catalytic activity of a new acidic ordered mesoporous silica (SBA-15)

Kayvan Habibi^a, Manouchehr Mamaghani^{a,b,*}, Mohammad Nikpassand^a

^aDepartment of Chemistry, Islamic Azad University, Rasht Branch, Rasht, Iran.

^bDepartment of Chemistry, Faculty of Sciences, University of Guilan, P.O. Box 41335-1914, Rasht, Iran.

Received 20 May 2018; received in revised form 27 August 2018; accepted 8 October 2018

ABSTRACT

SBA-15 is an interesting mesoporous silica material having highly ordered nanopores and a large surface area, which is widely employed as a catalyst. This mesoporous silica due to silanol groups is easily functionalized by various organic materials. A new acidic ordered functionalized mesoporous silica (SBA-15-Aminopropyl-Benzyl-SO₃H) has been introduced as an efficient catalyst for solvent-free esterification of fatty acids with ethanol. The structure of the catalyst and prepared materials have been characterized by FT-IR spectroscopy, XRD, thermogravimetric analysis (TGA), TEM, acid-base titration and NH₃-TPD techniques and N₂ adsorption-desorption isotherm. The high loading acidic sites with hydrophobic nature of the catalyst facilitate the esterification reaction in high yield without using special methodology. The results demonstrated that the reaction can also be performed in water as an environmentally benign and inexpensive solvent. The catalyst has been easily separated from the reaction mixture and used for at least six reaction runs without any significant loss of activity.

Keywords: SBA-15, Ordered mesoporous silica, Acidic catalyst, Catalytic activity, Palmitic acid, Free fatty acids.

1. Introduction

Ordered mesoporous silica was first reported in 1992 by Beck and coworkers in Mobil petroleum company [1]. These materials have achieved increasing interest in their catalyst applications, because of their distinction in morphology control, pore size, and wall composition. [2-4]. During the last two decades, grafting molecular catalysts onto the pore walls of mesoporous silica has provided numerous applications ranging from material chemistry to catalysis [5]. Among all the ordered mesoporous silicas, SBA-15 silicas are the most frequently studied [6-10]. SBA-15 silica demonstrates interesting textural and structural properties, such as large specific surface areas (above 1000 m²/g), uniform pore size (in the range 4–30 nm), high pore volume, high surface-to-volume ratio, variable framework compositions, thermal and hydrothermal stability and thick framework walls [7-9]. For this reason, several solid acid catalysts based on ordered mesoporous materials with different pore sizes and surface properties have been prepared as a heterogeneous and recyclable

catalyst in the relatively wide range of important acid-catalyzed functional group transformation [11-14]. However, due to the intrinsic hydrophilicity of silica framework and also the high polarity of the grafted sulfonic acid group in these solid acids, they were deactivated via adsorption of water during the reactions in which water acted as a reaction partner (Fig. 1) [15].

Although this limitation can be relieved by modifying the surface of the catalyst to make it more hydrophobic, there is still a challenge to achieve more appropriate solid acid catalysts by emphasizing the possibility to control both acidity and hydrophobicity of the catalyst [16-18].

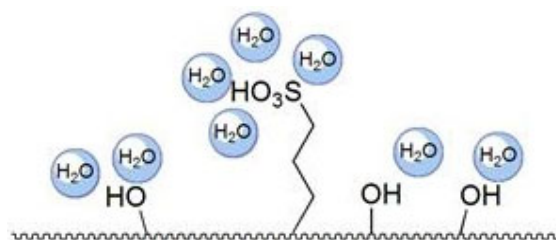


Fig. 1. Catalyst deactivation by adsorption of water on the surface of silica based sulfonic acid catalyst.

*Corresponding author.

E-mail address: m-chem41@guilan.ac.ir (M. Mamaghani)

Synthesis of fatty acid methyl/ethyl esters known as biodiesel has attracted special attention in the last decade [19] as they are a good replacement for fossil fuels to decrease the global energy crisis. The traditional way to biodiesel production is transesterification of triglycerides with a short-chain alcohol (such as methanol or ethanol) using NaOH as a base catalyst [20]. However, sodium hydroxide is a corrosive reagent and hence an additional neutralization step is required, leading to production of a high volume of salty waste. In addition, the residual free fatty acid (in the case of less expensive feedstock such as waste oil) is saponified by the homogeneous alkali catalyst, which increases the separation cost. In this regard, several fatty acids based on metal oxides (such as CaO and MgO) have been produced as heterogeneous solid catalysts [21]. However, the leaching of the active sites and low surface area are among the drawbacks of these routes which remain unresolved. Moreover, in some cases to achieve enough biodiesel products, the applied metal oxide should be mixed with strong bases such as MgO–KOH and MgO–NaOH systems [22].

Acid catalyst esterification is a promising way to solve the problems of the mentioned traditional base catalyst reactions. Esterification of the fatty acid with mesoporous silica–sulfonic acid can improve reaction efficiency, catalyst separation, and reusability [23-29].

In this study, we functionalized the surface of SBA-15 as ordered mesoporous silica through benzyl groups as an ionic liquid to increase the hydrophobicity of the surface of the silica. The authors proposed that a synergistic effect of the grafted sulfonic acid groups on the benzyl group and hydrogen sulfate counter anion of the supported ionic liquid assembled by hydrophobic nature of the catalyst is the main reason of the unnatural activity of the catalyst.

2. Experimental

2.1. Materials and equipment

All chemicals and solvents were purchased from the Sigma Aldrich and Merck and used without more purification. TLC was performed on silica gel 254 analytical sheets obtained from Fluka. The products were analyzed by an Agilent 7820A GC equipped with an FID detector, auto-sampler and Restek capillary column (Rtx®-50-DHA, 50 m, 0.20 mm ID, 0.5 mm). FT-IR spectra were recorded with ABB Bomem MB100 Fourier transform infrared analyzer. N₂ adsorption–desorption profiles were obtained using an Omnisorp-100 apparatus at 77 K and thermogravimetric analysis was performed by TGA-Q50. The low-angle XRD pattern was recorded on a Bruker diffractometer using

(Cu K α , λ = 1.5418 Å, 4 nm, 40 KV, 30 mA). HR-TEM was used to visualize the structure of SBA-15 and catalysts. It was performed on a Phillips Tecnai F20 200-kV microscope. NH₃ temperature-programmed desorption (NH₃-TPD) measurements recorded with a Micromeritics AutoChem HP 2950 was equipped with a thermal conductivity detector.

2.2. Preparation of SBA-15

In a typical synthesis by Stucky et al. [30,31], 4 g of Pluronic P123: EO₂₀PO₇₀EO₂₀ (M_{av} = 5800, from Aldrich) as the structure directing agent is dissolved under stirring in 80 g of 2 M HCl and 20 g of H₂O under stirring. After this, 8.8 g of tetraethyl orthosilicate (TEOS) is added at 35 °C for 20 h. Then, this aqueous solution of triblock copolymer and TEOS are kept under static conditions for 24 h for ageing at 80 °C. After cooling to room temperature, the resulting solid was recovered by filtration, washed in deionized water and ethanol for neutralization, and dried under ambient conditions. The solid was heated by calcination at 550 °C for 5 h with air to remove the residual organic template materials, yielding the final mesoporous SBA-15 materials.

2.3. Preparation of SBA-15-propyl-NH₂

SBA-15 as a silica source is prepared, then is functionalized with aminopropyl. First, the SBA-15 was activated by refluxing in 6 M hydrochloric acid (HCl) for 24 h. It was then washed thoroughly with the deionized water to adjust the pH of the solution to 6–7 (for neutralization) and dried at 100 °C for 24 h. The activated SBA-15 (2.5 g) was mixed with 5 mmol of (3-aminopropyl) triethoxysilane in the dry toluene for 24 h. The solid materials were then filtered off and washed with hot toluene for 48 h in a continuous extraction apparatus (Soxhlet) and dried in an oven at 100 °C for 24 h to give aminopropyl SBA-15 as a white solid product.

2.4. Preparation of the catalyst

A mixture of 2.0 g SBA-15-propyl-NH₂ and 5 mmol benzyl bromide was refluxed in dry toluene for 24 h. Then, the solids were filtrated off and washed with dry toluene (2 × 75 mL) and dried at 100 °C. Chlorosulfonic acid (10 mmol) was added to the solution of the prepared material in 50 mL of dry chloroform and the mixture was refluxed for 48 h [32]. Then, the solid material was filtrated and the residual chlorosulfonic acid was carefully washed with absolute ethanol several times. Finally, the material was exposed to 2M solution of H₂SO₄ at room temperature. After 12 h, the material was filtrated off and washed with diethyl ether and dichloromethane to obtain the catalyst.

2.5. Acidity measurements of Catalyst (SBA-15-Aminopropyl-Benzyl-SO₃H)

Temperature-programmed desorption of ammonia (NH₃-TPD) was used to determine the total acidity of the samples. Before the adsorption of ammonia, a sample was pretreated at 423 K for 2 h in a flow of ultrapure argon gas, and then cooled to 323 K and several ammonia pulses were flushed through the sample tube. After saturation, weakly adsorbed NH₃ was removed by argon gas at the same temperature. The TPD experiments were performed in the temperature range of 323 to 673 K at a heating rate of 10 K/min under dry argon.

The total acid densities of the synthesized catalyst were determined by acid–base titration. 0.5 g of catalyst was added to an aqueous solution of NaCl (1 M, 25 mL) and the mixture was stirred for 24 h. After this time, the solid was separated from the solution by filtration. Then the filtrate was titrated to an end point at pH of 7 with 0.01 M NaOH. From the volume of titrant solution, the acid exchange capacity was determined in units of mequiv of H⁺/g of samples [33].

2.6. General procedure for fatty acid esterification with Catalyst (SBA-15-Aminopropyl-Benzyl-SO₃H)

Fatty acid (2 mmol), ethanol (2 mL) and the catalyst (10 mol %) were added to a 10 mL round-bottom flask equipped with a condenser and a magnetic stirrer. The mixture was heated to 70 °C in stirring conditions. The reaction progress was monitored by TLC and GC. After completion of the reaction, the slurry was filtrated and the catalyst was washed with n-hexane (2 × 25 mL) and was filtered off. The residual fatty acid in the organic phase was quenched with 5% aqueous solution of NaHCO₃ (2 × 4 mL). After evaporation of the solvent under reduced pressure, the mixture was dried over dry MgCl₂ and fatty acid ethyl ester (FAES) was obtained in high yield.

3. Results and Discussion

Ordered mesoporous silica materials such as SBA-15 possess excellent structural properties involving large surface area (S_{BET}), uniform pore size distribution (D_p), high pore volume (V_p) and tunable dimensionality of the pore channels and structural orderings. In addition, they have high surface silanol groups that ensure them being easily functionalized by active sites. These unique properties provide the functionalized ordered mesoporous silica materials with especial attractions in catalysis. Among various functionalized mesoporous silica materials, organosulfonic acid functionalized ordered silica materials have been extensively

investigated. They are the robust solid acids having a high Bronsted acid strength and the plentiful number of acid sites. They have demonstrated considerably high catalytic activity in a number of acid-catalyzed reactions such as esterification.

In this study, SBA-15 was prepared and then functionalized with propylamine and benzyl bromide and then resulting in material sulfonated with Chlorosulfonic acid and H₂SO₄ for the synthesis of the catalyst. All material after preparation were analyzed.

Ordered Mesoporous silica (SBA-15) was synthesized according to the literature procedure [22]. The final surface area, pore diameter, and pore volume were determined to be 1040 m² g⁻¹, 10.8 nm, and 1.03 cm³ g⁻¹, respectively. The functionalization of walls decreases the surface area, pore diameter and pore volume of the SBA-15 confirmed by N₂ adsorption-desorption plots (Table 1).

An acidic catalyst was simply prepared by grafting the propylamine precursor onto the high surface area SBA-15 (Fig. 2, A). This prepared material easily reacts with benzyl bromide to obtain surface-bonded ammonium bromide species (B). Chlorosulfonic acid and H₂SO₄ treatment of the material and washing were performed to achieve the catalyst as a dry and slightly creamy powder (Fig. 2).

Comparative FT-IR spectra of SBA-15, SBA-15-propyl-NH₂ (A) and the catalyst has shown in Fig. 3. The bands at 2852 and 2923 cm⁻¹ in the spectra of the (A) present C–H and N–H stretching frequencies in the surface bonded aminopropyl functionalities.

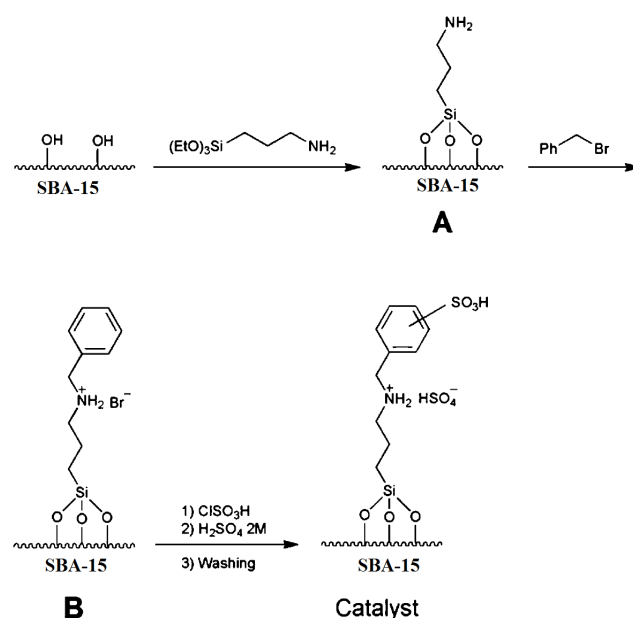


Fig. 2. Schematic illustration of the catalyst preparation.

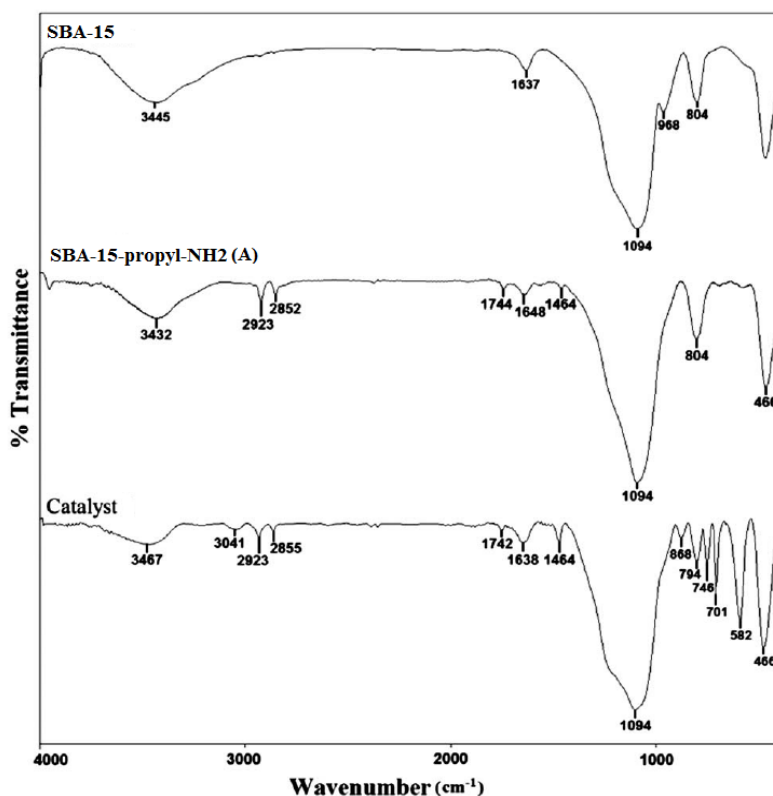


Fig. 3. FT-IR spectroscopy of the SBA-15, SBA-15- propyl-NH₂ (A) and the catalyst.

In the catalyst, another band at 3041 cm⁻¹ can be assigned to C–H stretching frequency of benzyl group moiety. The band at 582 cm⁻¹ with relatively high intensity is attributed to the S–O frequency of –SO₃H group. The double band frequency (S=O) of –SO₃H group seems to overlap with the broadband of the SBA-15 around the 1100 cm⁻¹.

For more evaluation about the structure of the catalyst before and after acid treatment, N₂ adsorption-desorption analysis was performed for SBA-15-propyl-NH₂ (A), SBA-15- propyl-NH₂-Benzyl (B) and catalyst (Fig. 4, Table 1). SBA-15 was protected by aminopropyl groups to the synthesis of material A inside the pores. From the N₂ sorption analysis, the decrease of the BET surface area from 1042 to 755 m²/g, the pore volume from 1.03 to 0.92 cm³/g, and the pore size from 10.8 to 4.8 nm confirmed the successful coating of aminopropyl groups onto the channel surfaces of pristine SBA-15 (green curve). N₂ adsorption/desorption isotherm of the material B is shown in the Fig. 4 (black curve). BET (Brunauer–Emmett–Teller) surface area of the material B was decreased from the initial (material A) 755 m² /g to 664 m²/g (material B). Moreover, the pore volume of the material B was reduced from the initial (material A) 0.92 cm³/g to 0.83 cm³/g (material B).

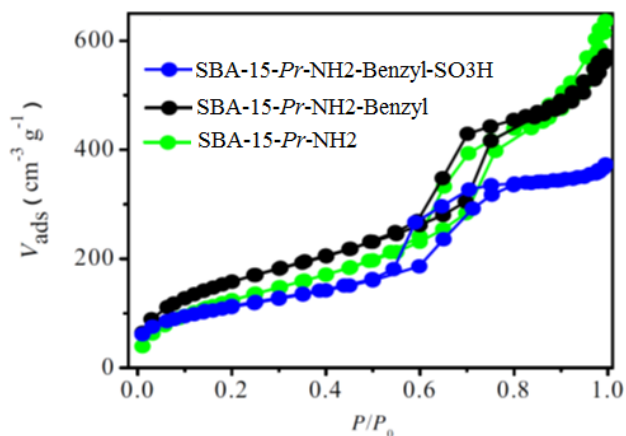


Fig. 4. Nitrogen adsorption–desorption isotherms of various functionalized SBA-15.

Table 1. Structural parameters of prepared materials.

Entry	S _{BET}	D _p (nm)	V _p (cm ³ /g)
SBA-15	1040	10.8	1.03
SBA-15-Aminopropyl (A)	755	6.6	0.92
SBA-15-Aminopropyl-Benzyl (B)	664	5.7	0.83
SBA-15-Aminopropyl-Benzyl-SO ₃ H (Catalyst)	380	4.8	0.54

The mean pore diameter of the catalyst was calculated to be 6.4 nm derived from the BJH (Barrett–Joyner–Halenda) average pore diameter analysis. The decrease in surface area and the pore volumes in the N₂ adsorption–desorption analysis of the material B clearly proved that the benzyl groups were supported onto the channels of the mesoporous material A. The results demonstrate the type IV adsorption-desorption isotherm over the range $P/P_0 = 0.5–0.8$ with 2H hysteresis loop for synthesis catalyst (blue curve). The BET surface area of the catalyst was found to be 380 m²/g. The value of the mean pore diameter of catalyst was derived from the adsorption branch of BJH (Barrett–Joyner–Halenda) average pore diameter analysis and was calculated to be 4.8 nm. Further information for prepared material and intermediate is shown in Table 1.

Mesostructure and morphology of SBA-15 and various functionalized SBA-15, as well as the catalyst, are characterized by low-angle XRD measurement (Fig. 5). This analysis demonstrates that all tested samples exhibit three well-resolved peaks at 0.80 (intense), 1.36 (weak) and 1.59 (weak) degree, which are respectively indexed as the (100), (110) and (200) reflections of the 2D hexagonal structure. The results show that the characteristic mesostructure of SBA-15 silica is retained after the functionalization of aminopropyl, benzyl and sulfonate groups into the SBA-15 walls.

TEM images of SBA-15 and catalyst are shown in Fig. 6. This image confirmed characteristic mesostructure of prepared SBA-15 and catalyst.

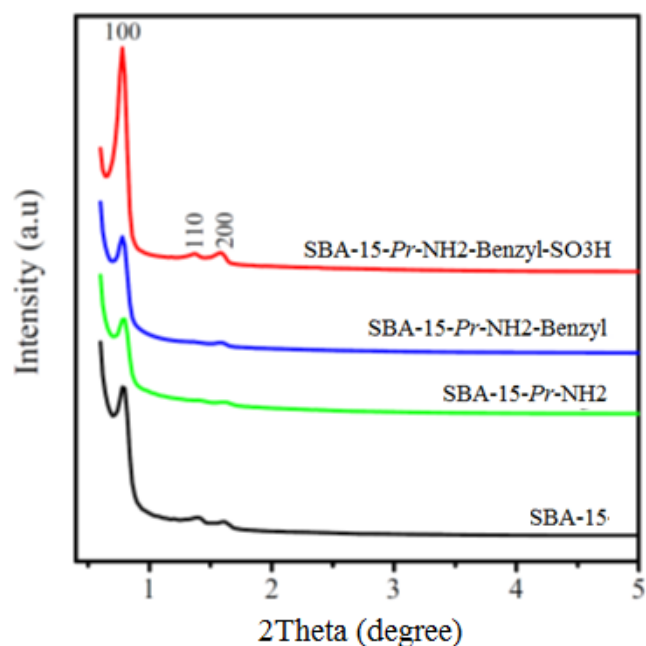


Fig. 5. Low-angle XRD patterns of various functionalized SBA-15 silica materials and SBA-15.

A comparison of the TEM images of the catalyst and the SBA-15 also indicates that the both synthesized materials have 2D-hexagonal (honeycomb) nanostructures, but after functionalization of SBA-15, the pore size has been reduced, this was confirmed by the BET analysis.

Fig. 7 showed the NH₃-TPD curve obtained for the catalyst (SBA-15-Aminopropyl-Benzyl-SO₃H). The TPD spectra of NH₃ from the SBA-15-SO₃H materials showed a low-temperature peak and a high temperature peak at ca. 443 K and ca. 600 K to 673 K respectively. Therefore, all the SBA-15-SO₃H materials showed two peaks in the NH₃-TPD curves which are attributed to desorption of NH₃ from weak acid sites and from medium strong acid sites [34].

NH₃ temperature-programmed desorption (NH₃-TPD) was used to determine the total acidity of the acidic catalyst. The NH₃-TPD profiles demonstrate two peaks in the range of 323–673 K. The peaks around 363 and 593 K can be attributed to desorption of NH₃ from the weak (–OH in SBA-15 surface that unreacted with functional groups) and moderately strong (–SO₃H) Brønsted acid sites in catalyst, respectively.

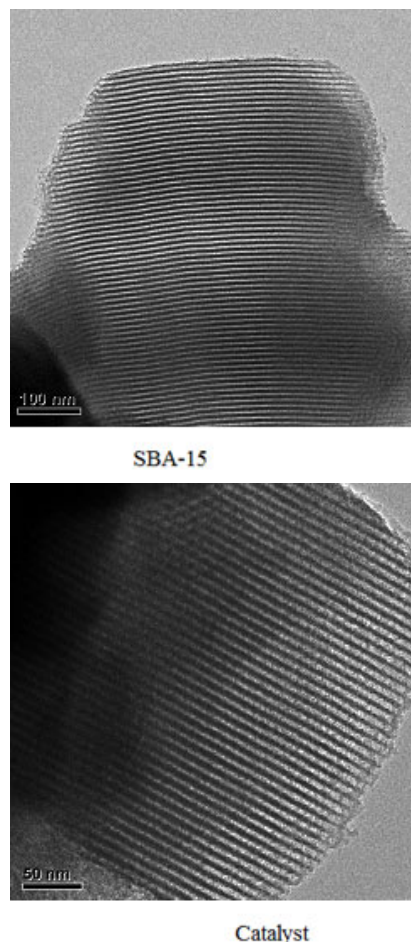


Fig. 6. TEM images of SBA-15 and the catalyst.

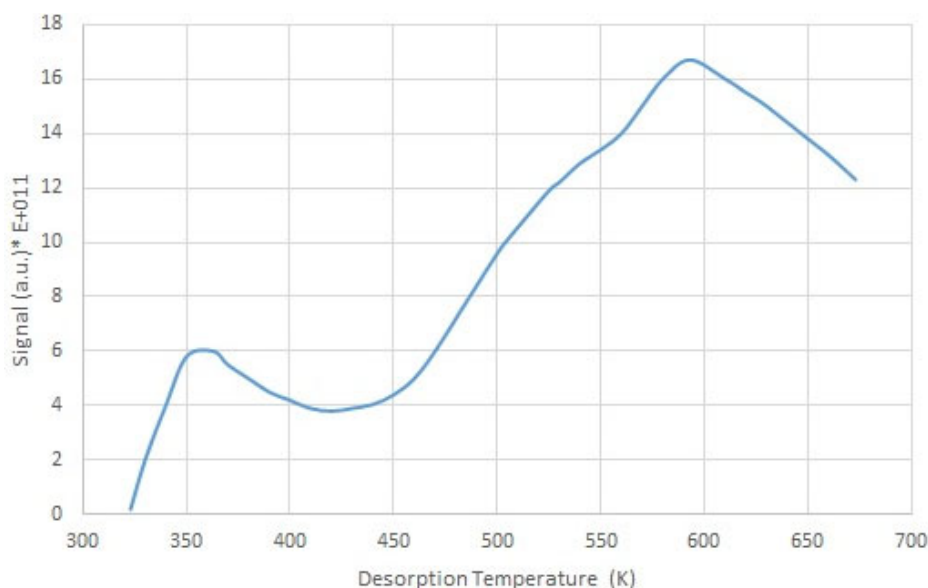


Fig. 7. NH_3 -TPD curve for the catalyst (SBA-15-Aminopropyl-Benzyl- SO_3H).

Ion exchange pH analysis was performed for the catalyst with 1 M solution of NaCl according to the known literature procedures [33]. The result of the experiment indicated that the loading of the catalyst is approximately $1.55 \text{ mmol H}^+ \text{ g}^{-1}$.

Thermogravimetric analysis (TGA) show the significant thermal stability for BSEA-SBA-15. The result has been given in Fig. 8. As shown in Fig. 8 no detectable weight loss could be assigned up to 200°C in the thermogram of the catalyst. But typically, the presence of water in the silica-based catalyst is explained as a presence of a sharp weight loss which usually occurs around 100°C in TGA of the catalyst. This observation can be interpreted

from the fact that the surface of the mesoporous silica modified with organic groups has a high degree of scheme hydrophobicity. The largest weight loss (34.86% and 8.15%) from 250 to 750°C in two-step is due to the degradation process of the grafted propyl and benzyl on SBA-15.

This hydrophobicity has two important effects on the esterification reaction: (i) the functionalized SBA-15 does not have a tendency to absorb water and thus no significant deactivation of the catalyst occurs during the reaction (ii) it facilitates mass transfer of organic starting material and simultaneously throws out water byproducts in the esterification reaction [18].

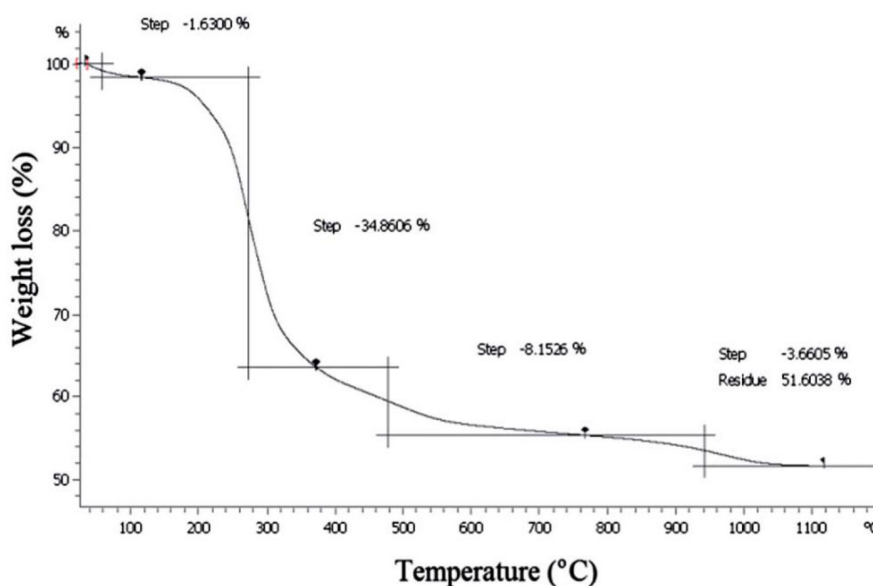


Fig. 8. TGA of the catalyst.

The performance of catalyst was initially investigated for esterification of the palmitic acid with ethanol. After preliminary investigation, we observed that an isolated yield of 64% of the ester product has been obtained when 10 mol% of the catalyst was used at room temperature for 48 h (Table 2, entry 1). When the reaction was performed at 70 °C, it produced the corresponding ester in 96% yield (Table 2, entry 2). When 10 mol% of catalyst was used at 70 °C (Table 2, entries 3–5), the FAES known as biodiesel was achieved in high yield. To study the effect of solvent, the reaction was performed in water, toluene and acetonitrile (Table 2, entries 6–9). Our investigation demonstrated that the esterification reaction can proceed well in water (Table 2, entries 6 and 7). In this regard, we found that high yield (84%) of ester was obtained at 90 °C after 12 h by an excess catalyst amount equal to 15 mol%. In this condition, the supported organic groups provide a hydrophobic environment in water.

Temperature has a significant effect on conversion of free fatty acids (FFA) such as palmitic acid to ethyl ester. After increasing temperature, the palmitic acid conversion was increased. At a certain temperature, the conversion was higher. In Fig. 9, the effect of the temperature on conversion of FFA (palmitic acid) was investigated and the results are represented. From the Fig. 9, it can be seen that the conversion was 96 % at the temperature higher than 60 °C temperature. Further increasing of temperature, the FFA does not increase conversion. The optimum temperature was 70 °C to complete other FFA.

Table 2. The results of catalytic performance for esterification of carboxylic acid with ethanol.

Entry	Acid	Solvent	Yield ^a (%)
1	Palmitic acid	-	64 ^b
2	Palmitic acid	-	96
3	Lauric acid	-	85
4	3-Phenylpropionic acid	-	83
5	Stearic acid	-	80
6	Palmitic acid	H ₂ O	51 ^c
7	Palmitic acid	H ₂ O	84 ^d
8	Palmitic acid	CH ₃ CN	23 ^c
9	Palmitic acid	Toluene	17 ^c

^aYields refer to isolated pure products in the presence of 10 mol% of proton equivalent of a weighted sample of prepared catalyst at 70 °C for 12 h and 2 mL ethanol.

^bThe reaction was performed at room temperature for 48 h.

^c1.5 mL of solvent was used in each case.

^d15 mol% of catalyst was used.

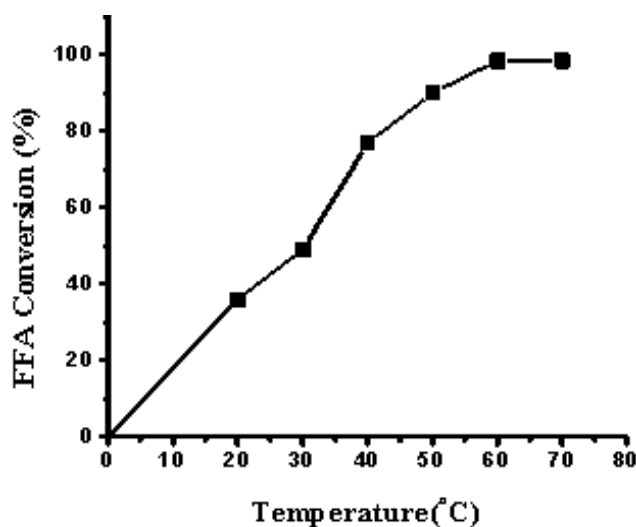


Fig. 9. Effect of temperature on palmitic acid conversion.

The recovery and reusability of catalyst were investigated for esterification of palmitic acid with ethanol at the optimized reaction condition (fatty acid, solvent and temperature). Therefore, after the first run of reaction, the mixture has been filtrated off and the catalyst was recovered. After drying, nearly 96% of the initial weighted catalyst was recovered. The recovered material was used in another reaction with identical conditions. The results show that catalyst exhibits similar catalytic activity for at least six times (The yields were 95, 94, 93, 92, 91 and 90 %, respectively) without any significant loss of efficiency.

In Table 3, we compare our study with other studies using another acid catalyst. These results show that the yield calculated in this study is higher than that previously reported for acid heterogeneous catalysts. In this work, we recovered and reused the catalyst 6 times, this demonstrates that the catalyst had better performance.

4. Conclusions

In summary, we design synthesis and characterization of a new acidic ordered mesoporous silica (SBA-15) with a commercial precursor for the esterification reaction. The high loading acidic sites with hydrophobic nature of the catalyst facilitate esterification reaction in high yield without using special methodology. The results demonstrated that the reaction can also be performed in water as an environmentally benign and inexpensive solvent. The catalyst has been easily separated from the reaction mixture and used for at least six reaction runs without significant loss of activity.

Table 3. Comparison of reaction condition and results of previous works with acid catalysts.

Entry	Catalyst	Fatty acid	Alcohol	Yield	Recovery	Ref.
1	20%PW/ZrO ₂	oleic acid	Trimethylolpropane	84 %	2 times	[35]
2	Nb ₂ O ₅ /SBA-15	castor oil	Methanol	80 %	5 times	[36]
3	Ga-Zn/Al-SBA-15	tall	Methanol	86 %	2 times	[37]
4	MoZn/Al-SBA-15	tall	Methanol	92 %	2 times	[37]
5	Al-SBA-15	Tricaprylin + 20 wt. % palmitic acid	Methanol	87.4 %	-	[38]
6	MCM-41-SO ₃ H	olive-pomace oil	monoacylglycerols (GMO + GMP)	40 %	3 times	[39]
7	SBA-15-aminopropyl-Benzyl-SO ₃ H	Palmitic acid	Ethanol	96 %	6 times	This work

References

- [1] C.T. Kresge, M.E. Leonowicz, W.J. Roth, J.C. Vartuli, J.S. Beck. *Nature* 359 (1992) 710-712.
- [2] J.Y. Ying, C.P. Mehnert, M.S. Wong. *Angew. Chem. Int. Ed.* 38 (1999) 56-77.
- [3] F. Schüth. *Chem. Mater.* 13 (2001) 3184-3195.
- [4] Y. Wan, D. Zhao. *Chem. Rev.* 107 (2007) 2821-2860.
- [5] G. Aragay, F. Pino, A. Merkoci. *Chem. Rev.* 112 (2012) 5317-5338.
- [6] Y. Han, D. Zhang. *Curr. Opin. Chem. Eng.* 1 (2012) 129-137.
- [7] W.J. Stevens, K. Lebeau, M. Mertens, G. Van Tendeloo, P. Cool, E.F. Vansant. *J. Phys. Chem. B* 110 (2006) 9183-9187.
- [8] F. Zhang, Y. Yan, H. Yang, Y. Meng, C. Yu, B. Tu, D. Zhao. *J. Phys. Chem. B* 109 (2005) 8723-8732.
- [9] N. Rahmat, A.Z. Abdullah, A.R. Mohamed. *Am. J. Appl. Sci.* 7 (2010) 1579-1586.
- [10] C.I. Léon, D. Song, F. Su, S. An, H. Liu, J. Gao, Y. Guo, J. Leng. *Microporous Mesoporous Mater.* 204 (2015) 218-225.
- [11] I.K. Mbaraka, D.R. Radu, V.S. Lin, B.H. Shanks. *J. Catal.* 219 (2003) 329-336.
- [12] N. Gokulakrishnan, A. Pandurangan, P.K. Sinha. *J. Mol. Catal. A: Chem.* 263 (2007) 55-61.
- [13] J.A. Melero, L.F. Bautista, G. Morales, J. Iglesias, R. Sánchez-Vázquez. *Chem. Eng. J.* 161 (2010) 323-331.
- [14] Q. Yang, M.P. Kapoor, S. Inagaki, N. Shirokura, J.N. Kondo, K. Domen. *J. Mol. Catal. A: Chem.* 230 (2005) 85-89.
- [15] B. Karimi, M. Vafaezadeh. *RSC Adv.* 3 (2013) 23207-23211.
- [16] B. Karimi, D. Zareyee. *Org. Lett.* 10 (2008) 3989-3992.
- [17] A. Corma, M. Renz. *Angew. Chem. Int. Ed.* 46 (2007) 298-300.
- [18] C.H. Tsai, H.T. Chen, S.M. Althaus, K. Mao, T. Kobayashi, M. Pruski, V.S. Lin. *ACS Catal.* 1 (2011) 729-732.
- [19] J.A. Melero, J. Iglesias, G. Morales. *Green Chem.* 11 (2009) 1285-1308.
- [20] F. Ma, M.A. Hanna. *Bioresour. Technol.* 70 (1999) 1-5.
- [21] Q. Zhang, H. Su, J. Luo, Y. Wei. *Green Chem.* 14 (2012) 201-208.
- [22] M. Manriquez-Ramírez, R. Gómez, J.G. Hernández-Cortez, A. Zúñiga-Moreno, C.M. Reza-San Germán, S.Q. Flores-Valle. *Catal. Today.* 212 (2013) 23-30.
- [23] J.A. Melero, L.F. Bautista, G. Morales, J. Iglesias, R. Sánchez-Vázquez. *Chem. Eng. J.* 161 (2010) 323-331.
- [24] Y. Wu, Z. Li, C. Xia. *Ind. Eng. Chem. Res.* 55 (2016) 1859-1865.
- [25] K. Saravanan, B. Tyagi, H.C. Bajaj. *Appl. Catal. B* 192 (2016) 161-170.
- [26] H. Pan, H. Li, X.F. Liu, H. Zhang, K.L. Yang, S. Huang, S. Yang. *Fuel Process. Technol.* 150 (2016) 50-57.
- [27] Y. Cao, H. Zhou, J. Li. *Renewable Sustainable Energy Rev.* 58 (2016) 871-875.
- [28] V. Benessere, M.E. Cucciolo, R. Esposito, M. Lega, R. Turco, F. Ruffo, M. Di Serio. *Fuel* 171 (2016) 1-4.
- [29] X. Zhang, F. Su, D. Song, S. An, B. Lu, Y. Guo. *Appl. Catal. B* 163 (2015) 50-62.
- [30] D. Zhao, J. Feng, Q. Huo, N. Melosh, G.H. Fredrickson, B.F. Chmelka, G.D. Stucky. *Science* 279 (1998) 548-552.
- [31] D. Zhao, Q. Huo, J. Feng, B.F. Chmelka, G.D. Stucky. *J. Am. Chem. Soc.* 120 (1998) 6024-6036.
- [32] M. Karaki, A. Karout, J. Toufaily, F. Rataboul, N. Essayem, B. Lebeau. *J. Catal.* 305 (2013) 204-216.
- [33] M. Vafaezadeh, M.M. Hashemi, M. Shakourian-Fard. *Catal. Commun.* 26 (2012) 54-57.
- [34] Y. Zheng, X. Su, X. Zhang, W. Wei, Y. Sun. *Stud. Surf. Sci. Catal.* 156 (2005) 205-212.
- [35] K.V. Avramidou, F. Zaccheria, S.A. Karakoulia, K.S. Triantafyllidis, N. Ravasio. *Mol. Catal.* 439 (2017) 60-71.
- [36] C. García-Sancho, R.M. Saboya, J.A. Cecilia, A.V. Sales, F.M. Luna, E. Rodríguez-Castellón, C.L. Cavalcante Jr. *Mol. Catal.* 436 (2017) 267-275.
- [37] J. Kocik, A. Samikannu, H. Bourajoini, T.N. Pham, J.P. Mikkola, M. Hájek, L. Čapek. *J. Clean Prod.* 155 (2017) 34-38.
- [38] D.A. Cabrera-Munguia, H. González, A. Gutiérrez-Alejandre, J.L. Rico, R. Huirache-Acuña, R. Maya-Yescas, E. Rosa. *Catal. Today.* 282 (2017) 195-203.
- [39] F. Alrouh, A. Karam, A. Alshaghel, S. El-Kadri. *Arab. J. Chem.* 10 (2017) S281-286.